Inorg. Chem. **2007**, *46*, 5616–5624

Solvent-Dependent Resonance Raman Spectra of High-Valent Oxomolybdenum(V) Tris[3,5-bis(trifluoromethyl)phenyl]corrolate

Roman S. Czernuszewicz,*,† Vicky Mody,† Adelajda A. Zareba,† Marzena B. Zaczek,† Michał Gałęzowski,‡ Volodymyr Sashuk,‡ Karol Grela,‡ and Daniel T. Gryko*,‡

Department of Chemistry, University of Houston, Houston, Texas 77204-5003, and Institute of Organic Chemistry, Polish Academy of Sciences, Kasprzaka 44/52, 01-224 Warsaw, Poland

Received February 11, 2007

UV–visible, infrared (IR), and resonance Raman (RR) spectra were measured and analyzed for a high-valent molybdenum(V)–oxo complex of 5,10,15-tris[3,5-bis(trifluoromethyl)phenyl]corrole (**1**) at room temperature. The strength of the metal–oxo bond in **1** was found to be strongly solvent-dependent. Solid-state IR and RR spectra of **1** exhibited the $Mo^{V}{\equiv}O$ stretching vibration at $\nu(Mo^{V}O) = 969$ cm^{-1}. It shifted up by 6 cm^{-1} to 975 cm^{-1} in *n*-hexane and then gradually shifted to lower frequencies in more polar solvents, down to 960 cm^{-1} in dimethyl sulfoxide. The results imply that stronger acceptor solvents weaken the $Mo^{V}{\equiv}O$ bond. The 45-cm^{-1} frequency downshifts displayed by **1** containing an ^{18}O label in the molybdenum(V)–oxo unit confirmed the assignments for the observed IR and RR $\nu(Mo^{V}O)$ bands. The solvent-induced frequency shift for the $\nu(Mo^{V}O)$ RR band, measured in a series of 25 organic solvents ranging from *n*-hexane (AN = 0.0) to *N*-methylformamide (AN = 32.1), did not decrease in direct proportion to Gutmann's solvent acceptor numbers (ANs). However, a good linear correlation of the $\nu(Mo^{V}O)$ frequency was found against an empirical "solvent polarity" scale ($A + B$) of Swain et al. *J. Am. Chem. Soc.* **1983**, *105*, 502–513. A molecular association was observed between chloroform and oxomolybdenum(V) corrole **1** through $Mo{\equiv}O{\cdots}H/CCl_3$ hydrogen-bonding interactions. This association manifested itself as a shift of the $\nu(Mo^{V}O)$ RR band of **1** in $CDCl_3$ to a higher frequency compared to that in $CHCl_3$.

Introduction

Corroles, analogues of porphyrins that are one carbon shorter, emerged recently as an independent area of research.[1−6] Their coordination chemistry,[7−12] photophysics,[13,14] synthesis,[15−23] chemical transformations,[24,25] electrochemistry,[26] and other properties[27−32] have been studied in great detail. In particular, progress in the coordination chemistry of corroles[5,33] has led to their use as catalysts in hydrocarbon oxidations,[34−36] as well as to the controversy over the "innocence" of their tetrapyrrole core.[8,37−42]

* To whom correspondence should be addressed. E-mail: roman@uh.edu (R.S.C.), daniel@icho.edu.pl (D.T.G.).
†University of Houston.
‡Polish Academy of Sciences.

(1) Paolesse, R. In *The Porphyrin Handbook*; Kadish, K. M., Smith, K. M., Guilard, R., Eds.; Academic Press: New York, 2000; Vol. 2; pp 201−232.
(2) Montforts, F.-P.; Glasenapp-Breiling, M.; Kusch, D. In *Houben−Weyl Methods of Organic Chemistry*; Schaumann, E., Ed.; Thieme: Stuttgart and New York, 1998; Vol. E9d; pp 665−672.
(3) Gryko, D. T. *Eur. J. Org. Chem.* **2002**, 1735−1743.
(4) Guilard, R.; Barbe, J.-M.; Stern, C.; Kadish, K. M. In *The Porphyrin Handbook*; Kadish, K. M., Smith, K. M., Guilard, R., Eds.; Elsevier: New York, 2003; Vol. 18; pp 303−351.
(5) Gryko, D. T.; Fox, J. P.; Goldberg, D. P. *J. Porphyrins Phthalocyanines* **2004**, *8*, 1091−1105.
(6) Nardis, S.; Monti, D.; Paolesse, R. *Mini-Rev. Org. Chem.* **2005**, *2*, 355−372.
(7) Meier-Callahan, A. E.; Di Bilio, A. J.; Simkhovich, L.; Mahammed, A.; Goldberg, I.; Gray, H. B.; Gross, Z. *Inorg. Chem.* **2001**, *40*, 6788−6793.
(8) Gross, Z. *J. Biol. Inorg. Chem.* **2001**, *6*, 733−738.
(9) Ramdhanie, B.; Stern, C. L.; Goldberg, D. P. *J. Am. Chem. Soc.* **2001**, *123*, 9447−9448.
(10) Edwards, N. Y.; Eikey, R. A.; Loring, M. I.; Abu-Omar, M. M. *Inorg. Chem.* **2005**, *44*, 3700−3708.
(11) Joseph, C. A.; Ford, P. C. J. *J. Am. Chem. Soc.* **2005**, *127*, 6737−6743.
(12) Collman, J. P.; Wang, H. J. H.; Decréau, R. A.; Eberspacher, T. A.; Sunderland, C. J. *Chem. Commun.* **2005**, 2497−2499.
(13) Ding, T.; Alemán, E. A.; Modarelli, D. A.; Ziegler, C. J. *J. Phys. Chem. A* **2005**, *109*, 7411−7417.
(14) Ventura, B.; Degli Esposti, A.; Koszarna, B.; Gryko, D. T.; Flamigni, L. *New J. Chem.* **2005**, *29*, 1559−1566.
(15) Gross, Z.; Galili, N.; Saltsman, I. *Angew. Chem., Int. Ed.* **1999**, *38*, 1427−1429.
(16) Paolesse, R.; Nardis, S.; Sagone, F.; Khoury, R. G. J. *J. Org. Chem.* **2001**, *66*, 550−556.
(17) Briñas, R. P.; Brückner, C. *Synlett* **2001**, 442−444.
(18) Guilard, R.; Gryko, D. T.; Canard, G.; Barbe, J.-M.; Koszarna, B.; Brandès, S.; Tasior, M. *Org. Lett.* **2002**, *4*, 4491−4494.

10.1021/ic070275g CCC: $37.00
Published on Web 06/05/2007

Molybdenum complexes of corroles, although known for some time,[43] have only recently been intensively studied.[44,45] Currently, two different methods to incorporate molybdenum into the corrole core are known: $Mo(CO)_6$ in decalin at 200 °C[43,45] and $MoCl_4(THF)_2$ (THF = tetrahydrofuran) in CH_2Cl_2 at 40 °C.[44] X-ray crystallography of one of the molybdenum corroles revealed a highly domed ring with a very large out-of-plane metal displacement (0.73 Å).[45] Interestingly, regardless of the oxidation state of molybdenum in the starting material, oxomolybdenum(V) complexes are always obtained and easily identified using electron paramagnetc resonance. However, all attempts to prepare complexes with different oxidation states or with chlorine as an axial ligand failed.[44,45] Molybdenum corroles attracted attention as potential catalysts, as enzyme models, and as analogues of corresponding molybdenum porphyrins. The main purpose of this paper is to report the results of solvent-dependent resonance Raman (RR) spectroscopic investigations on a molybdenum(V)−oxo corrole complex, [((CF$_3$)$_2$Ph)$_3$Cor]Mo^V≡O [**1**; (CF$_3$)$_2$Ph = *p*-3,5-bis(trifluoromethyl)phenyl; Cor = corrole)]).[44]

RR spectroscopy has been very successful in the structural and electronic elucidation of transition-metal tetrapyrrolic systems because of strong enhancement of the tetrapyrrole core and π-axial ligand vibrations via coupling to the $\pi-\pi^*$ electronic transitions in the visible region.[46] However, in contrast to extensively studied biological, geological, and synthetic metalloporphyrin systems,[47−51] including high-valent metalloporphyrin oxides,[52−57] only sparse RR spectra have been reported for metallocorroles.[58−61] In particular, there appears to be only one such work on tetrapyrrole complexes of oxomolybdenum(V) published in 1979, in which Nakamoto and co-workers measured the RR spectra of Mo^{V}O(MEC) (MEC = 2,3,17,18-tetramethyl-7,8,12,13-tetraethylcorrole) and Mo^{V}O(OEP)(OMe) (OEP = octaethylporphyrin) in the solid state.[58] Both Mo^{V}O(MEC) and Mo^{V}O(OEP)(OMe) showed relatively strong RR bands at 950 and 910 cm^{-1}, respectively, in the 457.9-nm excitation spectra that have been assigned to the Mo^V−O stretching mode, ν(Mo^{V}O). However, no confirmation of such a band assignment had been obtained via the ^{18}O-isotope-edited vibrational spectra.

In the present work, we report the Fourier transform infrared (FT-IR; solid state) and RR spectra (both solid state and solution) for oxomolybdenum(V) *meso*-triarylcorrole **1** (Figure 1) at room temperature. The solution RR spectra were measured and analyzed in a wide range of different organic solvents in order to assess the solvent-induced frequency shifts (SIFSs) of the Mo^V−O stretch. The room-temperature UV−visible spectra of **1** in the same set of 25 solvents were also measured and compared. Vibrational assignment for the observed ν(Mo^{V}O) FT-IR absorption and RR scattering bands

(19) Barbe, J.-M.; Burdet, F.; Espinoza, E.; Gros, C. P.; Guilard, R. *J. Porphyrins Phthalocyanines* **2003**, *7*, 365−374.
(20) Geier, G. R. I.; Chick, J. F. B.; Callinan, J. B.; Reid, C. G.; Auguscinski, W. P. *J. Org. Chem.* **2004**, *69*, 4159−4169.
(21) Jeandon, C.; Ruppert, R.; Callot, H. J. *Chem. Commun.* **2004**, 1090−1091.
(22) Luguya, R. J.; Fronczek, F. R.; Smith, K. M.; Vicente, M. G. H. *Tetrahedron Lett.* **2005**, *46*, 5365−5368.
(23) Koszarna, B.; Gryko, D. T. *J. Org. Chem.* **2006**, *71*, 3707−3717.
(24) Saltsman, I.; Mahammed, A.; Goldberg, I.; Tkachenko, E.; Botoshansky, M.; Gross, Z. *J. Am. Chem. Soc.* **2002**, *124*, 7411−7420.
(25) Paolesse, R.; Nardis, S.; Venanzi, M.; Mastroianni, M.; Russo, M.; Fronczek, F. R.; Vicente, M. G. H. *Chem.−Eur. J.* **2003**, *9*, 1192−1197.
(26) Shen, J.; Shao, J.; Ou, Z. E. W.; Koszarna, B.; Gryko, D. T.; Kadish, K. M. *Inorg. Chem.* **2006**, *45*, 2251−2265.
(27) DiNatale, C.; Salimbeni, D.; Paolesse, R.; Macagnano, A.; DAmico, A. *Sens. Actuators, B* **2000**, *65*, 220.
(28) Barbe, J. M.; Canard, G.; Brandès, S.; Jérôme, F.; Dubois, G.; Guilard, R. *Dalton Trans.* **2004**, 1208−1214.
(29) Radecki, J.; Stenka, I.; Dolusic, E.; Dehaen, W.; Plavec, J. *Comb. Chem. High Throughput Screening* **2004**, *7*, 375−381.
(30) Balazs, Y. S.; Saltsman, I.; Mahammed, A.; Tkachenko, E.; Golubkov, G.; Levine, J.; Gross, Z. *Magn. Reson. Chem.* **2004**, *42*, 624−635.
(31) Kadish, K. A.; Shao, J.; Ou, Z.; Frémond, L.; Zhan, R.; Burdet, F.; Barbe, J. M.; Gros, C. P.; Guilard, R. *Inorg. Chem.* **2005**, *44*, 6744−6754.
(32) Mahammed, A.; Gross, Z. *J. Am. Chem. Soc.* **2005**, *127*, 2883−2887.
(33) Erben, C.; Will, S.; Kadish, K. M. In *The Porphyrin Handbook*; Kadish, K. M., Smith, K. M., Guilard, R., Eds.; Academic Press: New York, 2000; Vol. 2; pp 233−300.
(34) Simkhovich, L.; Mahammed, A.; Goldberg, I.; Gross, Z. *Chem.−Eur. J.* **2001**, *7*, 1041−1055.
(35) Gross, Z.; Gray, H. B. *Adv. Synth. Catal.* **2004**, *346*, 165−170.
(36) Aviv, I.; Gross, Z. *Synlett* **2006**, 951−953.
(37) Zakharieva, O.; Schunemann, V.; Gerdan, M.; Licoccia, S.; Cai, S.; Walker, F. A.; Trautwein, A. X. *J. Am. Chem. Soc.* **2002**, *124*, 6636−6648.
(38) Ghosh, A.; Steene, E. *J. Inorg. Biochem.* **2002**, *91*, 423−436.
(39) Simkhovich, L.; Goldberg, I.; Gross, Z. *Inorg. Chem.* **2002**, *41*, 5433−5439.
(40) Walker, F. A.; Licoccia, S.; Paolesse, R. *J. Inorg. Biochem.* **2006**, *100*, 810−837.
(41) Kerber, W. D.; Goldberg, D. P. *J. Inorg. Biochem.* **2006**, *100*, 838−857.
(42) Ghosh, A. *J. Biol. Inorg. Chem.* **2006**, *11*, 712−724.
(43) Murakami, Y.; Matsuda, Y.; Yamada, S. *Chem. Lett.* **1977**, 689−692.
(44) Sashuk, V.; Koszarna, B.; Winiarek, P.; Gryko, D. T.; Grela, K. *Inorg. Chem. Commun.* **2004**, *7*, 871−875.
(45) Luobeznova, I.; Raizman, M.; Goldberg, I.; Gross, Z. *Inorg. Chem.* **2006**, *45*, 386−394.
(46) Czernuszewicz, R. S. In *Methods in Molecular Biology*; Jones, C., Mulloy, B., Thomas, A. H., Eds.; Humana: Totowa, NJ, 1993; Vol. 17; pp 345−374.
(47) *Biological Applications of Raman Spectroscopy*; Spiro, T. G., Ed.; Wiley: New York, 1988; Vol. 3.
(48) Spiro, T. G.; Czernuszewicz, R. S.; Li, X.-Y. *Coord. Chem. Rev.* **1990**, *100*, 541−571.
(49) Procyk, A. D.; Bocian, D. F. *Annu. Rev. Phys. Chem.* **1992**, *43*, 465−496.
(50) Kincaid, J. R. In *The Porphyrin Handbook*; Kadish, K. A., Smith, K. M., Guilard, R., Eds.; Academic Press: New York, 2000; Vol. 7; pp 225−291.
(51) Czernuszewicz, R. S.; Spiro, T. G. In *Inorganic Electronic Structure and Spectroscopy*; Solomon, E. I., Lever, A. B. P., Eds.; Wiley-Interscience: New York, 1999; Vol. 1; pp 353−442.
(52) Bajdor, K.; Nakamoto, K. *J. Am. Chem. Soc.* **1984**, *106*, 3045−3046.
(53) Proniewicz, L. M.; Bajdor, K.; Nakamoto, K. *J. Phys. Chem.* **1986**, *90*, 1760−1766.
(54) Su, Y. O.; Czernuszewicz, R. S.; Miller, L. A.; Spiro, T. G. *J. Am. Chem. Soc.* **1988**, *110*, 4150−4157.
(55) Czernuszewicz, R. S.; Su, Y. O.; Stern, M. K.; Macor, K. A.; Kim, D.; Groves, J. T.; Spiro, T. G. *J. Am. Chem. Soc.* **1988**, *110*, 4158−4165.
(56) Macor, K. A.; Czernuszewicz, R. S.; Spiro, T. G. *Inorg. Chem.* **1990**, *29*, 1996−2000.
(57) Czarnecki, K.; Proniewicz, L. M.; Fujii, H.; Ji, D.; Czernuszewicz, R. S.; Kincaid, J. R. *Inorg. Chem.* **1999**, *38*, 1543−1547.
(58) Ohta, N.; Scheuermann, W.; Nakamoto, K.; Matsuda, S.; Yamada, S.; Murakami, Y. *Inorg. Chem.* **1979**, *18*, 457−460.
(59) Steene, E.; Wondimagegn, T.; Ghosh, A. *J. Phys. Chem. B* **2001**, *105*, 11406−11413.
(60) Steene, E.; Wondimagegn, T.; Ghosh, A. *J. Inorg. Biochem.* **2002**, *88*, 113−118.
(61) Wasbotten, I. H.; Wondimagegn, T.; Ghosh, A. *J. Am. Chem. Soc.* **2002**, *14*, 8104−8116.

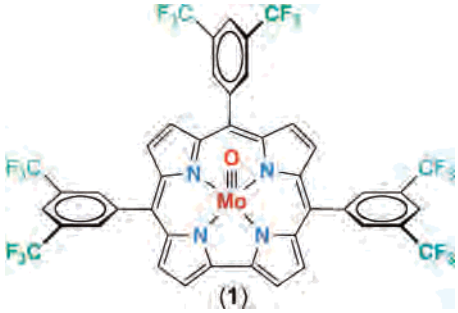

Figure 1. Structural diagram of oxomolybdenum(V) corrole **1**.

of **1** was made with the aid of $^{16}O/^{18}O$-isotope substitution at the oxo group. The influence of the solvents on the $Mo^{V}-O$ bond strength in oxomolybdenum(V) corrolate **1** was readily monitored with RR spectroscopy. The solid-state FT-IR (KBr pellet) and RR (KCl pellet) spectra of [$Mo^{16}O$]-**1** exhibited an intense $\nu(Mo^{V}O)$ vibrational band at 969.0 cm^{-1} that shifted by -45 cm^{-1} to lower frequency in the corresponding [$Mo^{18}O$]-**1** spectra. In the RR spectra of **1**, dissolved in cyclohexane, dichloromethane, and chloroform, the analogously ^{18}O-sensitive $\nu(Mo^{V}O)$ bands occurred at 974.5, 964.0, and 963.8 cm^{-1}, respectively. Such high frequencies of the $\nu(Mo^{V}O)$ stretch are consistent with the presence of a triply bonded $Mo^{V}\equiv O$ unit in **1**. The resonance-enhanced $\nu(Mo^{V}O)$ mode in solutions exhibited strong solvent dependence, with $\nu(Mo^{V}O)$ frequencies varying from 975.4 cm^{-1} in *n*-hexane (Gutmann's solvent AN = 0.0)[62] to 961.9 cm^{-1} in *N*-methylformamide (AN = 32.1) and 959.9 cm^{-1} in dimethyl sulfoxide (AN = 19.3). However, in contrast to the $V^{IV}-O$ stretching mode of vanadyl β-octaalkyl- and *meso*-tetraarylporphyrins ($3d^1$ metal−oxo systems),[54] a plot of the $\nu(Mo^{V}O)$ frequency against the Gutmann solvent ANs did not give a straight line for the molybdenum(V)−oxo *meso*-triarylcorrole **1**, a $4d^1$ metal−oxo species. A good linear correlation of the $\nu(Mo^{V}O)$ frequency was found for **1** by using a two-parameter "solvent polarity" scale ($A + B$) of Swain and co-workers, based on the sum of anion (A) and cation (B) solvation parameters derived from solvent effects on chemical reactivity.[63] This study yields a detailed solvent-dependent characterization of the high-valent $[((CF_3)_2Ph)_3Cor]Mo^{V}\equiv O$ complex.

Experimental Section

All chemicals were used as received unless otherwise noted. Reagent- or spectroscopic-grade solvents were distilled from appropriate drying agents prior to use. The free base of 5,10,15-tris[3,5-bis(trifluoromethyl)phenyl]corrole was synthesized as described earlier.[64] The synthesis of the molybdenum(V) oxo complex **1** was achieved by refluxing the free base corrole with $MoCl_4(THF)_2$ and diisopropylethylamine in CH_2Cl_2 at 40 °C, followed by flash chromatography (silica eluted with 1:9 ethyl acetate/cyclohexane) and recrystallization from CH_2Cl_2/ethanol.[44] Isotopic labeling of the oxo group with ^{18}O was carried out by preparing a millimolar sample of **1** dissolved in cyclohexane (~0.5 mL) and equilibrating it with ~20 μL of pure $H_2{}^{18}O$ (97 atom % ^{18}O; Isotec, Miamisburg, OH) for 24 h at room temperature under a N_2 atmosphere. Periodic recording of in situ RR spectra of the mixture using the 457.9-nm excitation line monitored the progress of $^{16}O/^{18}O$ exchange. After the RR spectrum showed that >95% of ^{18}O was incorporated into **1** (24 h), the reaction was stopped and the solution was evaporated to dryness under a vacuum. The resulting [$Mo^{18}O$]-**1** solid samples were pressed into KBr and KCl pellets to record the solid-state FT-IR and RR spectra, respectively, or redissolved in cyclohexane, chloroform, and dichloromethane to record the solution RR spectra.

The RR spectra were obtained using lines from Coherent Inova K-2 Kr^+ (406.7 and 413.1 nm), Coherent Inova 90-6 Ar^+ (457.9 nm), and Liconix 4260 He−Cd (441.6 nm) ion lasers by collecting backscattered (135° illumination angle) photons from spinning samples in pressed KCl pellets (solid samples)[65] or in 5-mm NMR tubes (solution samples).[66] Sample concentrations in the pellets were ~1 mg of corrole/200 mg of salt. Solution concentrations were ~0.1 mM for all excitation lines. All spectra were recorded at room temperature with 15−150-mW laser power and 4−6-cm^{-1} slit widths under the control of a Spex DM 3000 microcomputer system using a scanning Raman instrument equipped with a Spex 1403 double monochromator (with a pair of 1800 grooves/mm gratings) and a Hamamatsu 928 photomultiplier detector, as described in detail elsewhere.[46] The spectrometer was advanced in 0.5-cm^{-1} increments with integration times of 1 s for all spectra. To improve the signal-to-noise ratio multiple scans (2−6) were collected and then averaged. For some spectra, the slowly sloping baselines were subtracted from the digitally collected spectra using *GRAMS/AI* (version 7.01) software package (Thermo Galactic, Inc.). IR spectra were measured in KBr pellets at room temperature with a Nicolet Avator 360 FT-IR spectrophotometer. Electronic absorption spectra (250−800 nm) were obtained on a Cary 50 spectrophotometer (Varian) in 0.1-mm quartz cuvettes using freshly distilled solvents. The concentration of **1** in each solvent was adjusted such that the maximum absorbance of the Soret band was about 1 absorbance unit. Resolution of the spectra was 0.5 nm. The UV−visible (350−625 nm) and RR spectra (900−1000 cm^{-1}) were fitted with a curve-fitting subroutine of the *GRAMS/AI* (version 7.01) software. *IGOR Pro* (version 4.0) software (Wave Metrics, Inc.) was used to prepare the spectral figures.

Results and Discussion

Electronic Absorption Spectra and Soret-State RR Signatures. The molybdenum(V)−oxo corrole **1** was first examined with electronic absorption spectroscopy over the range of 250−800 nm. The UV−visible spectra were recorded at room temperature in 25 organic aprotic solvents and were fitted with a computer deconvolution program in order to determine the wavelengths of the absorption bands. The results from the curve fits are compiled in Table 1 for the main bands in the 375−625-nm absorption region. Five representative UV−visible spectra in this spectral region are shown in Figure 2, which compares the spectra obtained from solutions of molybdenum(V)−oxo corrole **1** in *n*-hexane, cyclohexane, dichloromethane, benzene, and carbon disulfide. It can be seen there that distinctive single Soret and several *Q* absorption bands[44] in the violet and green−orange regions, respectively, characterize each solution of [$((CF_3)_2$-

(62) Gutmann, V. *The Donor−Acceptor Approach to Molecular Interactions*; Plenum: New York, 1978.
(63) Swain, G. C.; Swain, M. S.; Powell, A. L.; Alumni, S. *J. Am. Chem. Soc.* **1983**, *105*, 502−513.
(64) Gryko, D. T.; Koszarna, B. *Org. Biomol. Chem.* **2003**, *1*, 350−357.
(65) Czernuszewicz, R. S. *Appl. Spectrosc.* **1986**, *40*, 571−573.
(66) Walters, M. A. *Appl. Spectrosc.* **1983**, *37*, 299−300.

Table 1. Electronic Absorption Maxima (nm) and Mo^V−O Stretching Frequencies (cm^{-1}) of the Oxomolybdenum(V) Corrole **1** in 25 Organic Solvents

entry	solvent	AN[a]	$A + B$[b]	λ_{max}[c]	ν(MoO)[d]
1	*n*-hexane	0.0	0.00	**432.6**, 506.7, 535.3, 550.8, 574.3, 592.8	975.4 (7.2)
2	cyclohexane	0.0	0.09	**433.6**, 506.9, 535.8, 551.7, 574.7, 593.0	975.4 (7.3)
3	triethylamine	1.4	0.27	**432.8**, 508.9, 535.2, 550.2, 574.6, 593.1	972.0 (8.7)
4	diethyl ether	3.9	0.46	**432.4**, 505.7, 534.5, 550.8, 574.0, 592.0	970.0 (9.1)
5	tetrahydrofuran	8.0	0.84	**434.4**, 508.2, 535.1, 550.3, 574.9, 592.9	966.5 (9.5)
6	benzene	8.2	0.73	**437.7**, 510.2, 538.2, 553.2, 577.9, 595.7	966.0 (11.4)
7	tetrachloromethane	8.6	0.43	**436.2**, 509.4, 537.4, 554.3, 576.1, 595.2	971.9 (12.9)
8	ethyl acetate	9.3	0.79	**432.5**, 506.2, 534.5, 549.9, 574.5, 591.6	966.7 (10.3)
9	hexamethylphosphoroamide	9.8	1.07	**435.1**, 508.2, 535.4, 551.8, 575.4, 592.5	961.7 (10.9)
10	methyl acetate	10.7	?[e]	**431.9**, 506.2, 535.0, 548.5, 573.9, 591.3	965.8 (10.6)
11	acetone	12.5	1.06	**432.3**, 504.9, 533.9, 549.2, 574.5, 590.8	964.5 (10.5)
12	*N*,*N*-dimethylacetamide	13.6	1.23	**434.3**, 507.1, 534.9, 550.4, 575.5, 591.7	961.7 (12.2)
13	pyridine	14.2	1.20	**438.3**, 511.4, 537.8, 553.5, 578.1, 595.5	961.6 (13.1)
14	benzonitrile	15.5	1.16	**438.9**, 510.9, 538.5, 553.5, 578.7, 596.6	962.3 (14.2)
15	*N*,*N*-dimethyformamide	16.0	1.23	**430.9**, 507.3, 542.7, 560.2, 576.9, 591.9	961.6 (12.7)
16	1,2-dichloroethane	16.7	1.12	**435.2**, 507.6, 536.0, 551.1, 574.9, 593.8	964.4 (13.3)
17	propylene carbonate	18.3	?	**433.3**, 506.8, 536.2, 550.9, 574.7, 590.9	960.8 (15.5)
18	acetonitrile	18.9	1.22	**431.4**, 506.2, 534.3, 550.6, 573.7, 590.1	962.6 (11.2)
19	dimethyl sulfoxide	19.3	1.41	**436.0**, 507.7, 538.1, 552.0, 576.7, 593.0	959.9 (12.7)
20	dichloromethane	20.4	1.13	**435.8**, 509.4, 535.7, 551.0, 576.0, 594.0	964.0 (13.0)
21	nitromethane	20.5	1.31	**433.2**, 507.3, 534.7, 549.5, 574.5, 591.9	962.1 (11.9)
22	chloroform	23.1	1.15	**435.8**, 510.0, 536.1, 551.7, 576.8, 595.0	963.8 (17.6)
23	*N*-methylformamide	32.1	?	**433.6**, 511.2, 536.1, 551.7, 575.5, 593.4	961.9 (15.3)
24	toluene	?	0.67	**437.5**, 509.7, 537.8, 552.5, 577.8, 595.6	967.5 (11.0)
25	carbon disulfide	?	0.48	**442.5**, 512.5, 541.3, 557.2, 580.5, 599.5	967.2 (10.0)

[a] Solvent ANs (*acceptivities*) as determined ^{31}P NMR spectroscopically at 25 °C by Gutmann and co-workers.[62,70,71] [b] Empirical "solvent polarity" parameters ($A + B$) (A = the solvent's anion-solvating tendency or *acidity*, and B = the solvent's cation-solvating tendency or *basicity*), as developed by Swain and co-workers.[63] [c] Electronic absorption maxima from room-temperature UV−visible spectra, obtained by curve deconvolution of the 375−625-nm regions. The Soret bands are highlighted in bold. [d] Vibrational frequencies from room-temperature RR spectra (6-cm^{-1} slit widths) excited at 441.6 nm. Numbers in parentheses are the effective bandwidths (fwhm = full width at half-maximum in cm^{-1}) of the corresponding ν(MoO) RR bands, obtained from the curve fits. [e] ? = value unknown.

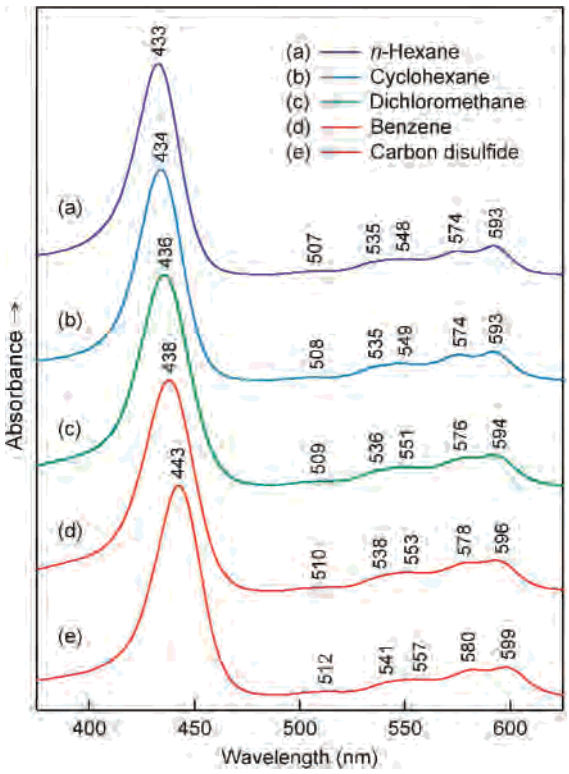

Figure 2. Room-temperature electronic absorption spectra of **1** in (a) *n*-hexane, (b) cyclohexane, (c) dichloromethane, (d) benzene, and (e) carbon disulfide.

Ph)$_3$Cor]Mo^V≡O. The *n*-hexane solution of **1** exhibits the Soret band at 432.6 nm (Figure 2a), which undergoes a red shift by ca. +1 to 433.5 nm, with **1** being dissolved in cyclohexane (Figure 2b). THF and *N*,*N*-dimethylacetamide shifted the Soret band by ca. +2 nm to longer wavelengths, while dimethyl sulfoxide, hexamethylphosphoroamide, and chlorinated solvents (tetrachloromethane, 1,2-dichloroethane, dichloromethane, and chloroform) all induced a slightly larger red shift of ca. +3 nm (Table 1), as exemplified by the spectrum in dichloromethane in Figure 2c. In comparison to the *n*-hexane solution, Table 1 and the UV−visible spectrum of the benzene solution in Figure 2d show that the largest bathochromic effect on the Soret band of molybdenum(V)−oxo corrole **1** is found for aromatic solvents and, surprisingly, carbon disulfide. Relative to the absorption maximum observed in *n*-hexane (~433 nm), the Soret band of **1** in benzene, toluene, pyridine, and benzonitrile is red-shifted by ca. +5 nm to ~438 nm and by nearly +10 nm to ~443 nm in carbon disulfide (Figure 2e). In general, similar bathochromic effects due to solvents discussed above were also found for the *Q* absorption bands in the 500−625-nm region (Table 1), again with the carbon disulfide solution exhibiting the greatest effect (ca. +7 nm; Table 1). On the other hand, the UV−visible spectra of **1** recorded in such solvents as diethyl ether, methyl and ethyl acetates, acetone, acetonitrile, and *N*,*N*-dimethylformamide all displayed slightly blue-shifted Soret as well as *Q* bands by ca. −0.5 to −2 nm when compared with the spectrum in *n*-hexane (Table 1). The *Q* absorption bands in the green−orange region in all of these solvents were comparable and also slightly blue-shifted relative to those seen in *n*-hexane. Finally, the results in Table 1 show that the electronic absorption bands of **1** dissolved in triethylamine match those observed in the *n*-hexane solution and that nitromethane, propylene carbonate, and *N*-methylformamide solutions of **1** absorb at nearly

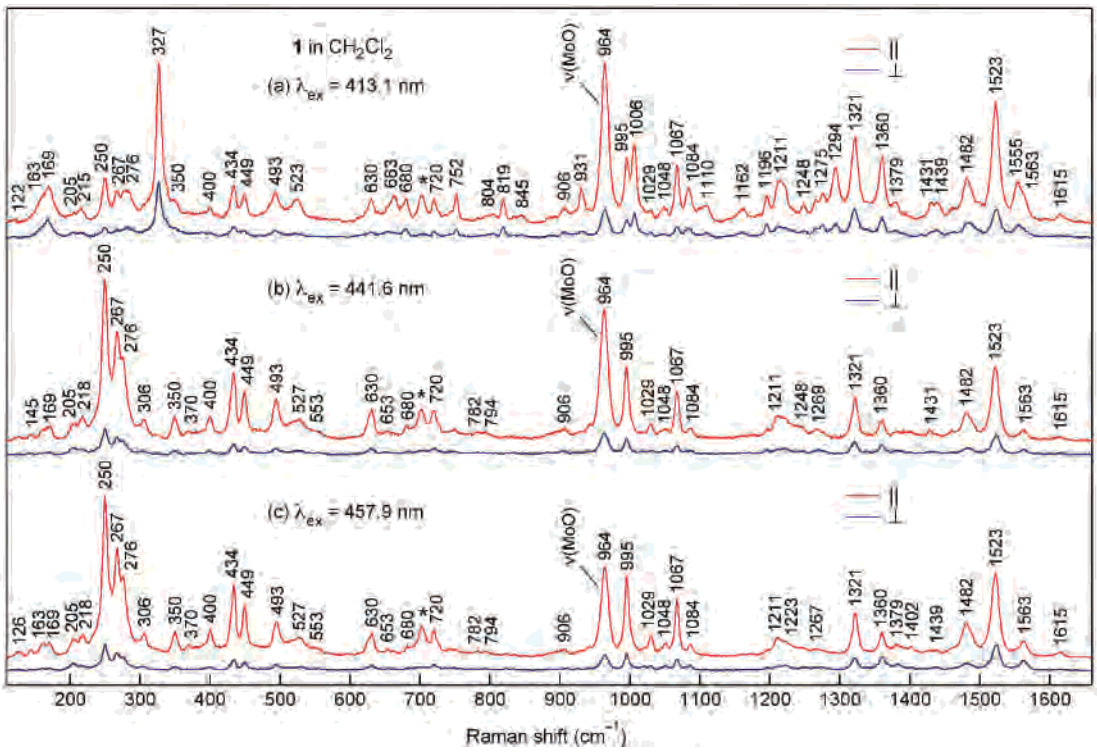

Figure 3. Soret-state RR spectra of **1** (≈1 mM) in dichloromethane in the 100−1675-cm^{-1} region, obtained with three indicated excitation wavelengths. Conditions: backscattering from a spinning NMR tube; ~100-mW laser power (~15 mW for a 441.6-nm line); 6-cm^{-1} slit widths; average of 2−4 scans, 1-s integration time at 0.5-cm^{-1} increments. Asterisks indicate dichloromethane solvent bands.

identical wavelengths as a cyclohexane solution, except for the *Q*-band region, where small differences do exist.

The molybdenum(V)−oxo corrole **1** dissolved well in all of the solvents listed in Table 1. All solutions of **1** were stable under the laser irradiation, allowing for high-quality RR spectra to be measured without any difficulties. Figure 3 shows the RR spectra in parallel (||) and perpendicular (⊥) scattering for the molydenum(V)−oxo corrole **1** in a dichloromethane solution in the 100−1670-cm^{-1} region obtained with excitation wavelengths at 413.1 (top), 441.6 (middle), and 457.9 (bottom) nm, in near-resonance with the Soret absorption band (~436 nm). All three excitation lines produce mainly *A*-term (Franck−Condon) scattering, which results in RR spectra that are dominated by polarized Raman peaks (p, with depolarization ratios, $\rho = I_{\perp}/I_{||}$, of <1/3) arising from totally symmetric vibrations.[46,67] The spectra excited at 457.9 and 441.6 nm are very similar in terms of their band frequencies and intensities (Figure 3b,c). A nearly identical and complex set of the same vibrational modes is also strongly enhanced by the 413.1-nm line (Figure 3a), but notable differences are quite apparent, particularly in the low-frequency region. The most striking difference occurs among the bands below 350 cm^{-1}, where an intense trio of p bands at 250, 267, and 276 cm^{-1} dominates the 457.9- and 441.6-nm excitation spectra. As Figure 3 demonstrates, these bands become dramatically weaker and a new p band appears very strongly at 327 cm^{-1} with a 413.1-nm excitation radiation. Besides the 327-cm^{-1} band, several additional p bands emerge in the 413.1-nm resonant spectrum at higher frequencies (663, 752, 1006, 1110, 1294, and 1555 cm^{-1}). Similar to the closely related metalloporphyrins, the in-plane stretching and deformation vibrations involving double C−C and C−N bonds of the corrole macrocycle should show the strongest increase in Raman intensity because of the interactions with the $\pi-\pi^*$ resonant electronic transitions, which are also polarized in the corrole plane. Although there is no doubt that this is the case for $[((CF_3)_2Ph)_3Cor]Mo^{V}{\equiv}O$, because its RR spectra exhibit a very rich array of strongly resonance-enhanced polarized Raman bands, no assignment to specific corrole skeletal vibrations can be made at this time because of the lack of a quantitative understanding of the corrole vibrational spectrum.

Nevertheless, Figure 3 demonstrates that one of the strongest polarized bands in the Soret-band-excited spectra of **1** in dichloromethane occurs at 964 cm^{-1}. This characteristic RR band has unequivocally been attributed to a stretching vibration of the $Mo^{V}-O$ bond, $\nu(Mo^{V}O)$, as described in detail below.

Identification of the $Mo^{V}-O$ Stretching Vibration, $\nu(Mo^{V}O)$. Vibrational spectroscopy can provide direct evidence for the $Mo^{V}-O$ bond through its characteristic stretching frequency in the IR and Raman spectra. Figure S-1a in the Supporting Information displays the 400−1650-cm^{-1} FT-IR spectrum of solid **1** in a KBr pellet. There are a few candidate bands in the 900−980-cm^{-1} region where the stretching vibration of the $Mo^{V}-O$ unit, $\nu(Mo^{V}O)$, is expected to occur,[58,68] and the moderately strong band at 969

(67) Czernuszewicz, R. S.; Maes, E. M.; Rankin, J. G. In *The Porphyrin Handbook*; Kadish, K. M., Smith, K. M., Guilard, R., Eds.; Academic Press: New York, 2000; Vol. 7; pp 293−337.

(68) Barraclough, C. G.; Lewis, J.; Nyhlom, R. S. *J. Chem. Soc.* **1959**, 3552−3555.

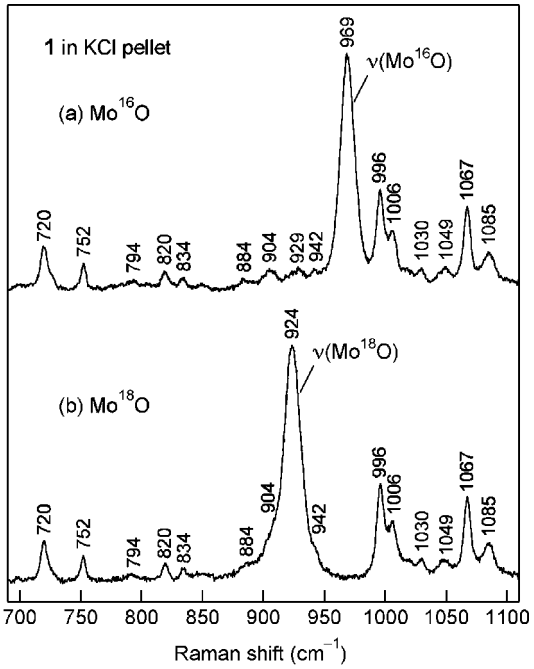

Figure 4. Effects of ^{18}O-isotope substitution on the 700−1100-cm^{-1} RR spectrum of solid **1** excited at 413.1 nm: (a) natural abundance **1** and (b) **1** substituted with ^{18}O at the oxo group. Conditions: backscattering from a spinning KCl pellet; ∼100-mW laser power; 4-cm^{-1} slit widths; average of 6 scans; 1-s integration time at 0.2-cm^{-1} increments.

cm^{-1} is assigned as the ν(Mo^{V}O) mode. A positive identification of the 969-cm^{-1} IR absorption band as the ν(Mo^{V}O) stretch comes from the solid-state RR spectrum of **1** in a KCl pellet (Figure S-1b in the Supporting Information), in which the ν(Mo^{V}O) mode gives rise to one of the strongest bands at 969 cm^{-1} when excited by the 441.6-nm line. More importantly, we attribute the 969-cm^{-1} band to the stretching vibration of the Mo^V−O unit because it shifts to 924 cm^{-1} when the oxo group in **1** is substituted with ^{18}O, as demonstrated in Figure 4. The observed ^{18}O-isotopic shift of ν(Mo^{V}O) (−45 cm^{-1}) is in very close agreement with that calculated for an isolated Mo−O diatomic oscillator (−47 cm^{-1}). Calculation of the force constant for the 969-cm^{-1} mode is a direct spectroscopic probe for a Mo^V≡O triple bond with the value of 7.58 mdyn/Å. This force constant is consistent with those calculated for the other known triply bonded, high-valent metal−oxo tetrapyrrole complexes.[51,69]

The solution RR spectra of isotopically labeled [Mo^{18}O]-**1** were recorded in three solvents, cyclohexane (AN = 0.0), dichloromethane (AN = 20.4), and chloroform (AN = 23.1), using excitation laser lines at 441.6 (cyclohexane) and 457.9 (CH_2Cl_2 and $CHCl_3$) nm. The results, which are compared to those of [Mo^{16}O]-**1** in Figure 5, demonstrate that dissolving [Mo^{16}O]-**1** in dichloromethane (middle panel) and chloroform (right panel) produces intense and broad ν(Mo^{V}O) RR bands (fwhm = 13.0 and 17.6 cm^{-1}, respectively) at lower frequencies, both at ∼964 cm^{-1}, than the 969-cm^{-1} band observed in the solid-state sample (Figure 4). When isotopically labeled [Mo^{18}O]-**1** is dissolved in dichloromethane and chloroform, the RR spectra display similar bands at ∼919 cm^{-1} in both solvents. The observed shifts by ∼45 cm^{-1} toward lower frequencies unequivocally validate the ν-(Mo^{V}O) vibrational assignment. In contrast, [Mo^{16}O]-**1** gives the ν(Mo^{V}O) band of markedly narrower width (fwhm = 7.2 cm^{-1}) at higher frequency, ∼974 cm^{-1}, when the RR spectrum is measured in cyclohexane (Figure 5, left panel). Again, the identity of the 974-cm^{-1} band in cyclohexane as the ν(Mo^{V}O) stretch is firmly established by the ^{18}O-isotopic shift to ∼928 cm^{-1} in the spectrum of [Mo^{18}O]-**1**.

SIFSs for the ν(Mo^{V}O) Stretch. The most obvious finding of the present RR study is that the Mo^V≡O bond of *meso*-triarylcorrole **1** is susceptible to solvent-induced polarization. Because of the polar character of the Mo^V≡O bond, it is possible for electron-donating and -accepting molecules to interact at the partially positive Mo and partially negative O ends, respectively. Both kinds of interactions are expected to weaken the Mo^V≡O bond by counteracting the $O^{2-} \rightarrow Mo^{5+}$ charge donation in the bond. In fact, Su et al. have previously published magnitudes of the SIFS involving a V^{IV}−O stretching RR band of vanadyl porphyrins and showed that polar solvents increase the SIFS in proportion to the electron acceptor strength.[54] In a series of 10 organic solvents, the ν(V^{IV}O) frequency decreased nearly linearly with increasing Gutmann's ANs,[62,70,71] from 1007 cm^{-1} in hexane (AN = 0.0) down to 982 and 992 cm^{-1} in chloroform (AN = 23.1) for VO(OEP) and VO(TPP) (TPP = *meso*-tetraphenylporphyrin), respectively.

Herein, we have measured the ν(Mo^{V}O) stretching RR band of corrole **1** in 25 aprotic organic solvents. Figure S-2 in the Supporting Information compares the resulting RR spectra in 21 solvents in the 925−1025-cm^{-1} region obtained with an excitation wavelength at 441.6 nm, sorted out (top to bottom) by the ascending Gutmann solvent ANs (Figure S-2a in the Supporting Information) and by the ascending Swain et al. solvent polarity parameters ($A + B$) (Figure S-2b in the Supporting Information). The frequencies are listed in Table 1 and plotted in parts a and b of Figure 6 against respectively the acceptor number AN and polarity parameter ($A + B$) of the solvent. Also listed in Table 1 are the observed effective bandwidths (fwhm = full width at half-maximum) for the ν(Mo^{V}O) RR bands in all considered solvents.

As expected, the *n*-hexane (AN = 0.0) solution of **1** produced the sharpest ν(Mo^{V}O) stretching RR band (fwhm = 7.2 cm^{-1}) at the highest frequency, 975.4 cm^{-1} (Table 1). In all other solvents, the ν(Mo^{V}O) band increased in width and decreased in frequency. The reduction in the ν(Mo^{V}O) vibrational frequency means that stronger acceptor solvents weaken the Mo^V−O bond by interacting with the electron pairs at the O end of the bond and impeding the O → Mo donation. However, Figure S-2a in the Supporting Information and Figure 6a clearly show that, unlike in the case of a ν(V^{IV}O) stretch of vanadyl porphyrins,[54] the SIFS for the ν(Mo^{V}O) RR band of molybdenum(V)−oxo corrole **1** are

(69) Mandimutsira, B. S.; Ramdhanie, B.; Todd, R. C.; Wang, H.; Zareba, A. A.; Czernuszewicz, R. S.; Goldberg, D. P. *J. Am. Chem. Soc.* **2002**, *124*, 15170−15171.

(70) Mayer, U.; Gutmann, V.; Gerger, W. *Monatsh. Chem.* **1975**, *106*, 1235−1257.

(71) Gutmann, V. *Electrochim. Acta* **1976**, *21*, 661−670.

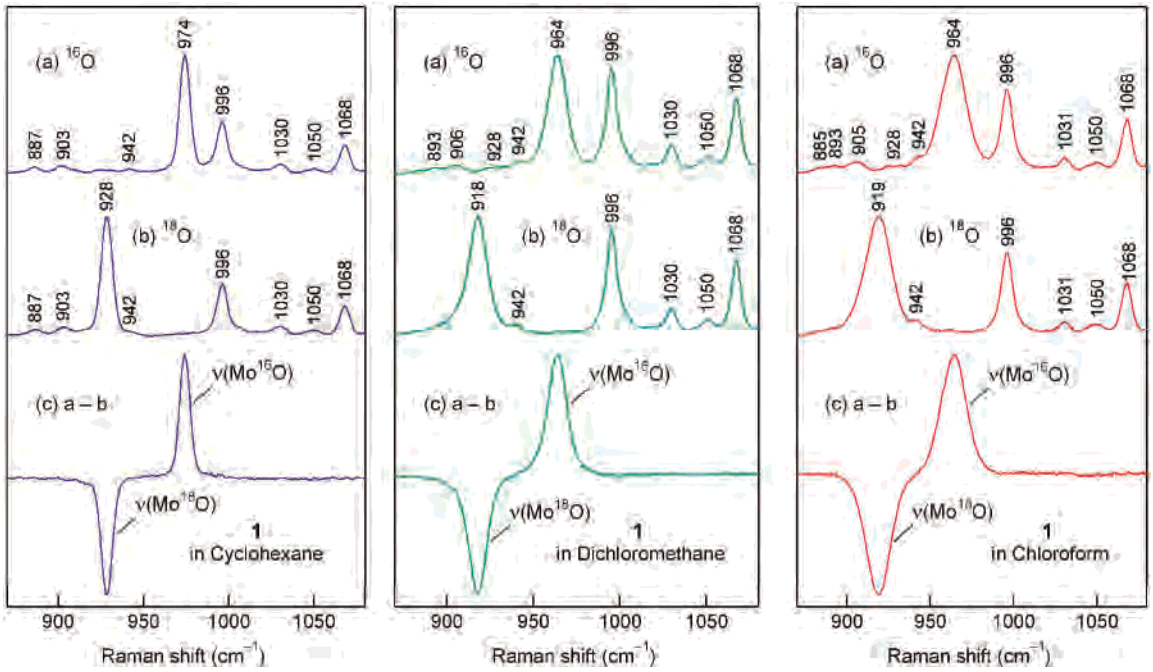

Figure 5. Effects of ^{18}O-isotope substitution on the 875−1075-cm^{-1} RR spectra of **1** in cyclohexane (left), dichloromethane (middle), and chloroform (right): (a) natural abundance **1**; (b) **1** substituted with ^{18}O at the oxo group; (c) corresponding (^{16}O − ^{18}O) difference spectra. Spectra were recorded at room temperature using excitation radiation at 441.6 nm (~15-mW laser power and 6-cm^{-1} slit widths) for a cyclohexane solution and 457.9 nm (~100-mW laser power and 6-cm^{-1} slit widths) for the dichloromethane and chloroform solutions, with 6-cm^{-1} slit widths and 1-s integration time at 0.2-cm^{-1} increments for all solutions (average of 6 scans).

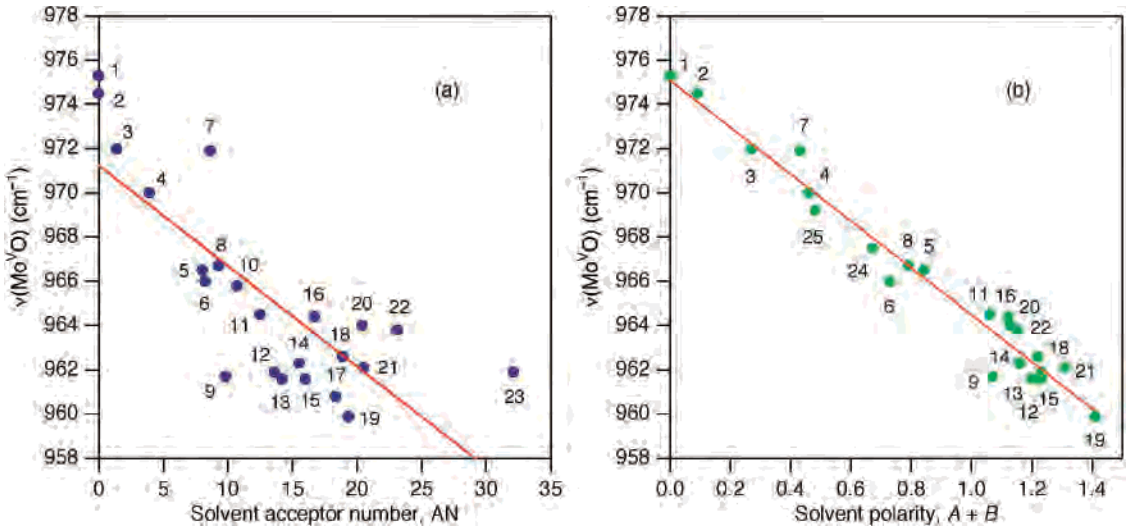

Figure 6. Plots of the ν(Mo^{V}O) frequency for **1** as a function of (a) solvent AN (23 data points)[71] and (b) solvent polarity parameter ($A + B$) (22 data points).[63]

not linearly correlated with the solvent's AN. In Figure 6a, a large scatter of the data points is quite apparent, especially among the solvents with AN greater than 8.5 (entries 7−23). Indeed, the equation of the least-squares fit is very poor, namely, ν(Mo^{V}O) = 971.24 − 0.45393AN, with a standard deviation of 1.15 cm^{-1} and a correlation coefficient of 0.7953 using data in 23 solvents (solvents 1−23, out of 25 listed in Table 1). Consequently, the electrophilic character of a solvent (as measured by the AN) cannot alone determine the SIFS magnitude for [((CF$_3$)$_2$Ph)$_3$Cor]Mo^{V}≡O.

On the other hand, in Figure S2-b in the Supporting Information and Figure 6b, a clear straight line emerges once the RR spectra and ν(Mo^{V}O) frequencies are sorted out by an ascending parameter ($A + B$), which is considered as a reasonable measure of the "solvent polarity" in terms of the overall solvation capability of a solvent.[63] The description of the solvent effect is then ν(Mo^{V}O) = 975.08 − 10.589($A + B$) using 22 solvents (solvents 1−9, 11−16, 18−22, 24, and 25 in Table 1). The standard deviation is reduced to 0.429 cm^{-1}, and the correlation coefficient is 0.9825.

Molecular Association between Chloroform and 1. One of the striking features of the RR spectra of **1** is the ν(Mo^{V}O) bandwidth that changes significantly with the solvent. Representative spectra are expanded in Figure 7, and the fwhm values are summarized in Table 1. As expected, noninteracting solvents such as *n*-hexane (Figure 7a−d) and

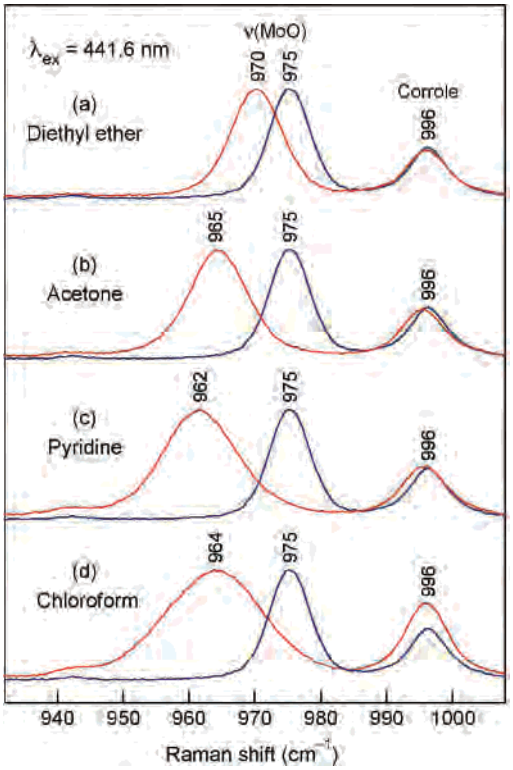

Figure 7. Expanded ν(Mo^{V}O) region of the 441.6-nm excitation RR spectra for **1** in (a) diethyl ether, (b) acetone, (c) pyridine, and (d) chloroform (red traces), showing the changes in the ν(Mo^{V}O) frequency and bandwidth due to the solvent relative to those in *n*-hexane (blue traces). The largely unaffected bands at ∼996 cm^{-1} arise from a corrole ligand vibration. Conditions: as in Figure 5.

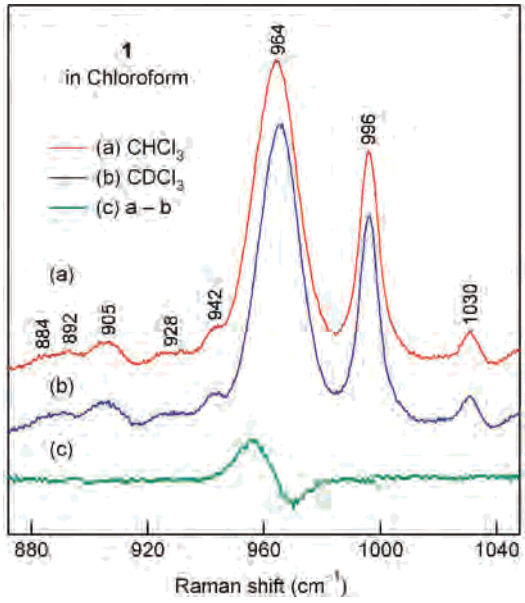

Figure 8. Expanded ν(Mo^{V}O) region of the RR spectra for **1** in (a) $CHCl_3$ and (b) $CDCl_3$ and their ($CHCl_3$ − $CDCl_3$) difference spectrum (c), showing the shifted ν(Mo^{V}O) mode (963.8 cm^{-1}) to a higher frequency (by +1.3 cm^{-1}) in deuterated chloroform. All other bands that cancel in the difference spectrum arise from corrole ligand vibrations. Conditions: backscattering from a spinning NMR tube; 457.9-nm excitation; ∼100-mW laser power; 6-cm^{-1} slit widths; average of 4 scans; 1-s integration time at 0.2-cm^{-1} increments.

cyclohexane produced the sharpest ν(Mo^{V}O) RR bands, with a bandwidth of ∼7.2 cm^{-1} (fwhm). Somewhat broader bands of ∼8.5−10.5 cm^{-1} were observed in such solvents as triethylamine, diethyl ether (Figure 7a), THF, methyl and ethyl acetates, carbon disulfide, and acetone (Figure 7b). The bandwidth increased to ∼11−13 cm^{-1} in the remaining solvents, except for benzonitrile, *N*-methylformamide, propylene carbonate, and chloroform (Figure 7d). In the latter four solvents, the ν(Mo^{V}O) RR bands were the broadest, with fwhm values of 14.4, 15.3, 15.5, and 17.6 cm^{-1}, respectively. Heterogeneity in the solvent environment due to strong associative effects existing in aprotic solvents[72] is no doubt responsible for much of these bandwidth variations, but specific solute−solvent interactions may also contribute.

Displayed in Figure 8 is the ν(Mo^{V}O) region of the 457.9-nm excitation RR spectra for **1** in $CHCl_3$ and $CDCl_3$ solvents together with their ($CHCl_3$ − $CDCl_3$) difference spectrum. Clearly, there is a shift of the ν(Mo^{V}O) stretching band (963.8 cm^{-1}) toward higher frequencies (by +1.3 cm^{-1}) on going from $CHCl_3$ to $CDCl_3$, implying a slight strengthening of the Mo^V≡O bond in the $CDCl_3$ solution. The remaining RR bands, which arise from corrole ligand modes, were unaffected, and all completely cancel in the difference spectrum (Figure 8c). We attribute this H/D sensitivity of the ν(Mo^{V}O) stretching frequency to a molecular association between chloroform and corrole **1** through specific Mo^V≡O···H/D/CCl_3 dipole−dipole, or hydrogen-bonding, interactions. A slightly higher ν(Mo^{V}O) frequency and, therefore, a slightly stronger Mo^V≡O bond for the **1**/$CDCl_3$ molecular complex compared to **1**/$CHCl_3$ is consistent with a smaller dipole moment of $CDCl_3$ (μ = 1.09 D) than that of $CHCl_3$ (μ = 1.14 D). $CDCl_3$, being a weaker dipole, is expected to polarize the Mo^V≡O bond less by withdrawing less electron density from the O atom and, therefore, to increase the ν-(Mo^{V}O) stretching frequency.

Chloroform has been classified as an apolar aprotic solvent, i.e., an organic solvent that is characterized by a low relative permittivity (ϵ_r = 1.15 D, <15), a low dipole moment (μ = 1.14 D, <2.5 D), a low E_T value (E_T = 0.259, <0.3), and the inability to act as a H-bond donor.[72] Apparently, our present experimental RR data for **1** in $CHCl_3$ and $CDCl_3$ indicate that the H−C bond in chloroform is sufficiently polarized to act as a H-bond donor by interacting with lone electron pairs on the O atom of the Mo^V≡O unit. In fact, a molecular association between gaseous chloroform and sulfur dioxide through CH···O hydrogen bonding has recently been detected by FT-IR spectroscopy by Chung and Hippler.[73]

Conclusions

UV−visible, IR, and RR spectroscopic studies on high-valent [((CF$_3$)$_2$Ph)$_3$Cor]Mo^V≡O (**1**) were performed. The key vibrational mode, ν(Mo^{V}O), was identified in both the solid state and solution by ^{18}O-isotope labeling of the terminal oxo ligand. This stretching vibration was strongly enhanced in resonance with the Soret electronic transition, and its frequency was sensitive to solute−solvent interactions that

(72) Reichardt, C. *Solvents and Solvent Effects in Organic Chemistry*; Wiley-VCH: Weinheim, Germany, 2003.

(73) Chung, S.; Hippler, M. *J. Chem. Phys.* **2006**, *124*, 214316−214322.

weaken the $Mo^{V}\equiv O$ triple bond by inhibiting $O^{2-} \rightarrow Mo^{5+}$ electron donation. The $\nu(Mo^{V}O)$ frequency, recorded in 25 aprotic organic solvents, decreased in proportion to a solvent polarity parameter ($A + B$) of Swain et al.,[63] but it did not follow in a linear fashion Gutmann's solvent ANs.[71] A molecular association between chloroform and **1** through $C-H\cdots O\equiv Mo^{V}$ hydrogen-bonding interactions was found to be present in solution and detected by RR spectroscopy.

Acknowledgment. The financial support from the Robert A. Welch Foundation (Grant E-1184 to R.S.C.), the Volkswagen Foundation, and the Polish Ministry of Science and Education (to D.T.G.) is gratefully acknowledged. We thank Tomasz J. Czernuszewicz for his technical assistance in the preparation of this manuscript.

Supporting Information Available: Figure S-1 showing FT-IR and RR spectra of solid **1** at room temperature and Figure S-2 showing the effects of 21 organic solvents on the $\nu(Mo^{V}O)$ RR band of **1**. This material is available free of charge via the Internet at http://pubs.acs.org.

IC070275G